Extending the Pressure–Temperature State Diagram of Myoglobin

by **Filip Meersman**[a]), **László Smeller**[b]), and **Karel Heremans***[c])

[a]) Department of Chemistry, University of Cambridge, Lensfield Road, Cambridge CB21EW, UK
[b]) Department of Biophysics and Radiation Biology, Semmelweis University, Puskin u. 9, PF 263, H-1444 Budapest
[c]) Department of Chemistry, Katholieke Universiteit Leuven, Celestijnenlaan 200D, B-3001 Leuven (phone: +32.16.32.71.59; fax: +32.16.32.79.82; e-mail: Karel.Heremans@fys.kuleuven.ac.be)

Dedicated to Professor *André E. Merbach* on the occasion of his 65th birthday

The pressure–temperature (*P*,*T*) diagram of proteins proposed by *Hawley* concerns the equilibrium between native and denatured forms. However, the importance of protein aggregation is increasingly recognized, and it has been suggested that certain aggregated states represent alternative folds of the polypeptide chain. Here, we present a *P*,*T*-diagram for myoglobin in which we include the aggregated state and suggest to call it a *P*,*T*-state diagram, as not all boundaries are true equilibrium transitions. We observe by *Fourier* transform infrared spectroscopy that increasing temperature causes the protein to aggregate, but that a subsequent further temperature increase results in the dissociation of this aggregate. Moreover, we observe that moderate pressures stabilize myoglobin against thermal denaturation. We hypothesize that this effect originates from the volume changes associated with the aggregation transition.

1. Introduction. – A physical description of a liquid or a substance requires one to consider both temperature and pressure as variables. Temperature variations change the volume and the thermal energy of the system, whereas pressure mainly affects the volume, enabling the determination of changes in partial molar volume and isothermal compressibility by pressure perturbation techniques [1]. The possible thermodynamic states of a compound can be depicted in a pressure–temperature (*P*,*T*) diagram. Water is a case in point, with its various ice isomorphs, which, at high pressure, have higher densities than that of ice (0.1 MPa) [2]. In 1903, *Tammann* suggested the possibility an elliptically shaped *P*,*T*-diagram [3]. Such a diagram has since been observed for the pressure–temperature-induced denaturation of proteins. Following the seminal observation on egg white by *Bridgman* [4], *Suzuki* [5] studied the denaturation kinetics of the proteins ovalbumin and carbonylhemoglobin as a function of temperature and pressure and found a dome-shaped curve reminiscent of the *Tammann* curve for crystal melting with the points of isokineticity connected. Similarly, *Hawley* [6] investigated the equilibrium denaturations of chymotrypsinogen and ribonuclease A and observed the re-entrant behaviour. The boundary of the ellipse is defined by the *P*,*T*-coordinates, where the *Gibbs* energy change for denaturation, $\Delta G = G_D - G_N$, is zero. Within the elliptic contour, the protein is in the native conformation ($\Delta G > 0$); outside the contour, the protein is denatured ($\Delta G < 0$). The intersection of the boundary with the temperature axis at lower temperatures indicates the cold denaturation of proteins and was predicted by *Brandts et al.* [7]. Elliptical diagrams

have also been observed for starch gelation [8], the inactivation of microorganisms [9][10], and polymers in the presence and absence of water [11][12].

Suzuki [5] found that, at temperatures below 30°, the kinetics of the pressure denaturation of carbonylhemoglobin and ovalbumin is characterized by negative activation entropy and enthalpy. Such negative activation energies have also been observed for the urea-induced denaturation of proteins. To explain his observations he proposed the following mechanism:

$$P + n\ H_2O \Leftrightarrow P(H_2O)_n \rightarrow P_D \quad (1)$$

where P is native protein, $P(H_2O)_n$ is hydrated protein, and P_D is denatured protein. Thus, he suggested that pressure induces the penetration of water into the protein, which subsequently denatures. More-recent experimental and computational observations support such a mechanism [13–15]. For example, *Jacob et al.* [16] demonstrated that water is required to overcome the activation barrier for the pressure denaturation of the cold-shock protein CspB. Solution conditions such as pH and the presence of cosolutes or chemical denaturants determine the size and position of the diagram [16–18].

Smeller [19] has pointed out that the thermodynamic description of the *P,T*-diagram suggested by *Hawley* [6] has a number of underlying assumptions. For instance, in its present state, the diagram is valid for reversible, two-state denaturation events and does not take into account the possible existence of intermediate or metastable states. As it is becoming increasingly recognized that protein aggregates represent alternative conformations with conformational stabilities comparable to that of the native state [20], it is of interest to explore the pressure–temperature regions where these aggregates are stable and to include them in the *P,T*-diagram. In addition, the *P,T*-diagram suggests that the denatured-state ensemble has the same properties throughout the pressure–temperature plane. The latter is not necessarily the case, as it has been shown that the pressure-, cold-, and heat-denatured states can be conformationally different [21–23].

Previously, we studied the cold-, heat-, and pressure-induced unfolding of myoglobin by *Fourier* transform infrared (FT-IR) spectroscopy [24]. The characterization of the heat-denatured state was obscured by the occurrence of protein aggregation. Here, we report the dissociation of the aggregate and subsequent analysis of the denatured state, thereby enabling us to characterize the denatured state at different pressure and temperature combinations. To reach the high temperatures to observe the dissociation, we performed pressure-assisted high-temperature experiments. The role of pressure is to prevent the solvent from evaporating at high temperature, as pressures of a few MPa are sufficient to keep water in the liquid state up to 200° [25]. Interestingly, we observe pressure-induced thermostabilization of the protein against aggregation at *ca.* 75°. These observations allow us to propose an extended *P,T*-diagram for myoglobin in which states other than the native and denatured states are taken into consideration and to discuss various features of the diagram.

2. Results. – 2.1. *Effect of Temperature on Myoglobin at Moderate Pressures* (< 100 MPa). At 25°, the main feature in the amide I′ band of myoglobin is an intense

band at *ca.* 1650 cm^{-1}, typical of the large α-helix content of this protein (*Fig. 1*) [24]. The intensity of this band remains constant up to 70°; above this temperature, the α-helix band gradually disappears, and, concomitantly, two new bands appear at 1618 and 1683 cm^{-1}. These are assigned to the formation of intermolecular β-sheet structure [26–28]. As the temperature is further increased, these bands start to disappear, suggesting dissociation of the aggregate. The dissociation is complete at 140°, and the resulting broad, featureless band is typical of a denatured state. The thermally induced dissociation of protein aggregates has previously been observed for a number of proteins, including ribonuclease A, lysozyme, and horseradish peroxidase [29][30]. In the case of lysozyme and ribonuclease A, we were able to demonstrate that the properties of the denatured state obtained after temperature-induced disaggregation are the same as those of the denatured state obtained under non-aggregating conditions. Here, we assume that the denatured state of myoglobin is representative of the denatured state that would have been observed without prior aggregation. The disaggregation is reversible upon cooling, as indicated by the re-appearance of the IR aggregation bands. The aggregation persists at 25° (data not shown).

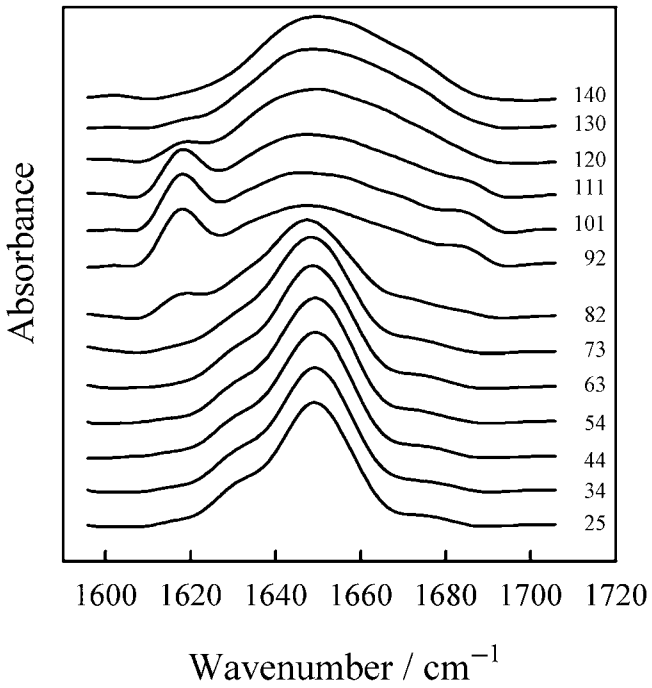

Fig. 1. *Pressure-assisted thermal scan of myoglobin: structural changes as observed in amide I′ band of the FT-IR spectrum.* Spectra are deconvoluted and computed with a linear baseline. Temperature in °.

Fig. 2 shows the evolution of the intensity of the band at 1618 cm^{-1}, characteristic of aggregation. The midpoints of the aggregation and dissociation transitions are $84.3 \pm 0.4°$ and $115.4 \pm 0.4°$, respectively. The midpoint of the aggregation transition is shifted by *ca.* 12° compared to our previous data at 0.1 MPa [24], suggesting that pressure

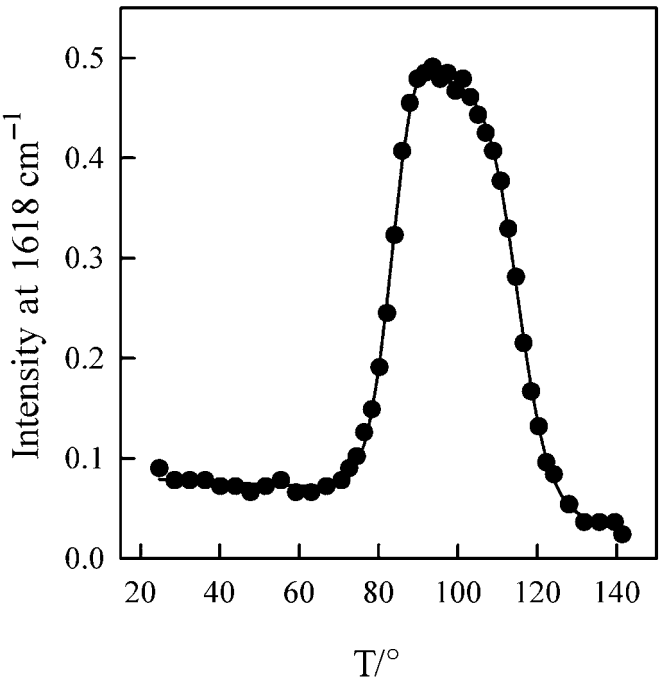

Fig. 2. *Intensity of the 1618 cm^{-1} band* vs. *temperature*. The band at *ca.* 1618 cm^{-1} is indicative of intermolecular aggregation.

stabilizes myoglobin against heat denaturation. The pressure at 84.3° was 89 MPa. This effect is reproducible, and it can be observed that, as the pressure decreases, the midpoint of the transition is shifted to lower temperature, whereas the dissociation transition is shifted to higher temperatures. For example, at 61 MPa the respective transition midpoints are 80° and 130°. Note that the pressure range in these experiments (< 100 MPa) is sufficiently low to assume that the dissociation is not a side effect of the applied pressure, as the dissociation of aggregates by pressure generally requires pressures of 200–300 MPa [31][32]. Moreover, previous observations of the dissociation of aggregates were made at 0.1 MPa [29][30]. However, as pressure is increased above this threshold, it is likely to prevent the aggregation. At that point, the aggregation and dissociation curves are expected to merge.

2.2. *Characterization of the Heat-Denatured State.* The secondary structure of the denatured state has been analyzed by curve-fitting (*Fig. 3*). It was found that seven Gaussian curves (at 1621, 1633, 1645, 1660, 1674, 1686, and 1695 cm^{-1}) contribute to the spectrum. The major bands at 1633 cm^{-1} (9.9%) and 1645 cm^{-1} (40.9%) have been assigned to extended chain and disordered structures, respectively [33][34], whereas the bands at 1660 cm^{-1} (35%) and 1674 cm^{-1} (12%) arise from turn and loop structures [27]. At high temperature, absorption bands at *ca.* 1665 cm^{-1} have also been assigned to irregular structures [35].

In *Fig. 4*, the spectra of the cold- and pressure-denatured states obtained previously are compared [24] with the denatured state after heat-induced dissociation. The latter

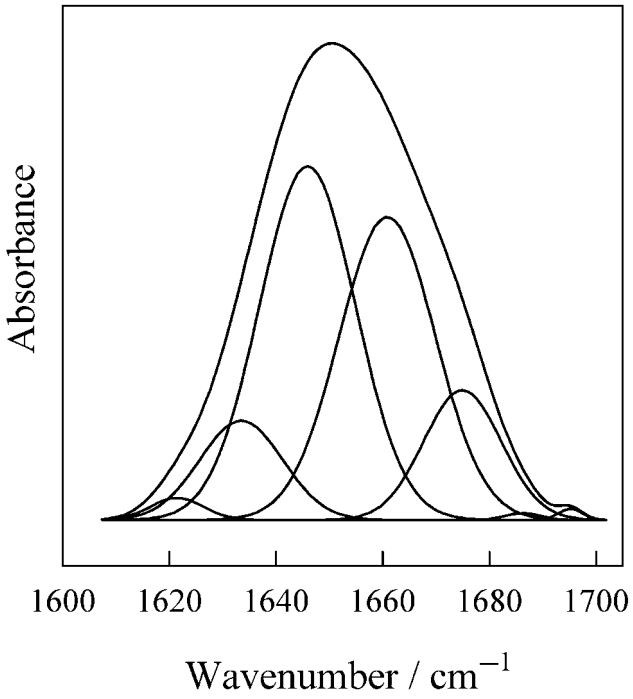

Fig. 3. *Characterization of the heat-denatured state of myoglobin.* Curve-fit of the deconvoluted amide I′ band obtained after temperature-induced dissociation of the aggregated protein (at 140° and 89 MPa).

distinguishes itself from the former two by a significantly lower amount of extended-chain structure (11% *vs.* 45–50%) and a higher degree of turn and loop structures (47%) above 1660 cm^{-1}. It is important to emphasize that the absence of a significant amount of β-sheet structure, which is generally the hallmark of a temperature-induced aggregate, is indicative of dissociation and the accompanying structural change. The area of the band at *ca.* 1645 cm^{-1} contributes to the spectrum to the same extent as in the case of the cold- and pressure-denatured states (*ca.* 40%). However, in the case of the heat denaturation, we have no reason to assume that there is still a contribution of α-helix to this band, as we did for the pressure and cold denaturation. This band is, therefore, indicative of disordered structure.

3. Discussion. – 3.1. *An Extended Pressure–Temperature-State Diagram for Myoglobin.* In the classical view of the protein *P,T*-diagram (reviewed by *Smeller* [19]), only the native and the denatured conformations are considered. However, it is now known that, whereas the native state represents a single conformation, the denatured state is a heterogeneous ensemble of unfolded conformations [36][37]. Thus, the question arises whether this heterogeneity exists throughout the *P,T*-space, or whether different denatured states exist under different conditions of pressure and temperature. In the present work, we have shown that the heat-denatured state is distinctly different from the cold- and pressure-denatured states characterized

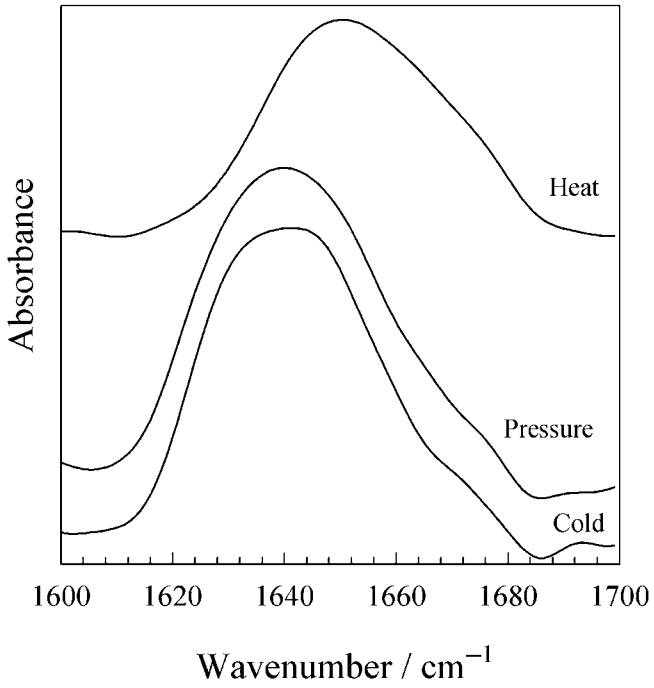

Fig. 4. *Comparison of cold-* (200 MPa and −25°) *and pressure-* (1.0 GPa and 25°) *denatured states of myoglobin with the heat-denatured state obtained after dissociation of the aggregate* (140° and *ca.* 89 MPa). The spectra of the cold- and pressure-denatured states were taken from [24].

previously [24]. This is in agreement with findings on ribonuclease A [22], β-lactoglobulin [21], thioredoxin h from *Chlamydomonas reinhardtii* [23], and *Streptomyces* subtilisin inhibitor [38].

The observed differences in thermodynamics of heat-, cold-, and pressure-denaturation imply that a conformational change is required to convert the heat-denatured state to the pressure- or cold-denatured states. *Tamura et al.* [38] showed that, in the case of *Streptomyces* subtilisin inhibitor, the transition between the heat- and cold-denatured states does not involve passage through the native state. Similar all-or-none transitions have also been observed between compact denatured states, such as the molten globule state, and the fully denatured state [39][40]. Taken together, these data could suggest the existence of additional boundaries in the elliptical *P,T*-diagram; one between the areas of the pressure- and heat-denatured states and another one between the cold- and heat-denatured states (*Fig. 5*). No boundary is suggested between the cold and pressure denatured states because of their conformational similarity [24]. The position of the broken line in *Fig. 5* has been arbitrarily chosen to coalesce with the ellipse axis where the volume change ΔV is zero, *i.e.*, where dP/dT changes sign. Above this line, ΔV is negative, and pressure significantly affects the properties of the denatured state. However, it has been suggested that the properties of the denatured state can also change continuously within the denatured domain

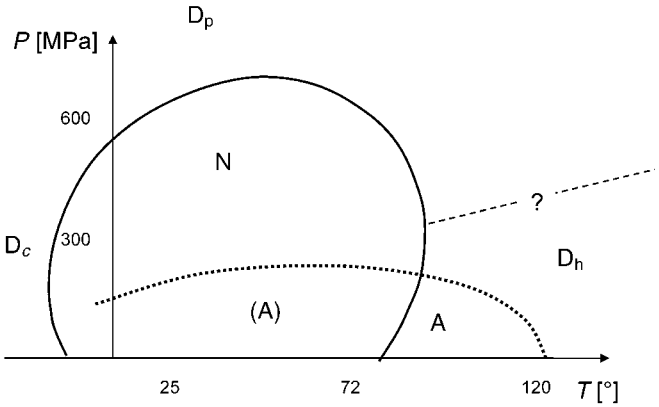

Fig. 5. *Pressure–temperature state diagram of myoglobin.* The heat- (D_h), cold- (D_c), and pressure-denatured (D_p) states, as well as the heat-induced aggregate (A_h) are indicated.

[19][41], and, therefore, a boundary does not necessarily exist. Thus, the exact outline of the diagram depends on the nature of the protein and the solvent conditions [16][17].

To represent the kinetic nature of some of the transitions between the different states, it would be more appropriate to consider the diagram as a state diagram. In this case, the *P,T*-space can be divided into separate domains in which different denatured conformations predominate. This is analogous to polymers, where true phase diagrams are rare [12]. Moreover, *Smeller* [19] pointed out the need for an extension of our present view of the *P,T*-diagram by including information on intermediate and possible metastable states. For instance, in a state diagram as suggested here, one can indicate under which *P,T*-conditions aggregates can exist. This is important for understanding of the interactions that drive protein aggregation [42]. Furthermore, the extended diagram proposed by *Smeller* [19] shows a linear division of the ellipse into regions below 200–300 MPa, where aggregates are stable, and above these pressures, where aggregates are usually dissociated. In view of our findings, we propose that this should be a curved line that intersects the temperature axis at high temperature (*Fig. 5*). The cooperativity of the dissociation transition suggests that a conformational change underlies this observation, in agreement with earlier work on lysozyme and ribonuclease A [30]. The transition of the aggregated state to the denatured state can, therefore, be considered to represent a true state boundary.

3.2. *On the Origin of the Pressure-Induced Thermostabilization.* The *P,T*-diagram of ribonuclease A reported by *Hawley* [6] shows a decrease in pressure stability with increasing temperature ($dP/dT < 0$ at T_m). In contrast, chymotrypsinogen shows a similar trend at higher pressures, but has increased thermal stability at moderate pressures ($dP/dT > 0$ at T_m below *ca.* 100 MPa). The mechanistic aspects underlying this phenomenon, called pressure-induced thermostabilization, are still elusive. *Hei* and *Clark* [43] suggested that the stabilization is correlated with the hydrophobicity of the protein, whereas *Heremans* [44] suggested a link with aggregation.

Here, we have shown that pressure stabilizes myoglobin against temperature-induced denaturation and concomitant aggregation. This is in contrast to the findings of *Zipp* and *Kauzmann* [17], who followed the changes in the absorbance of sperm whale myoglobin by UV/VIS spectroscopy at lower protein concentrations and found that dP/dT is negative at the T_m. This suggests that the shape of the diagram for a given protein can vary, in accordance with recent findings by *Dubins et al.* [40]. These authors found that pressure stabilizes the native state in the thermally induced native-to-denatured (N-to-D) transition of cytochrome c, whereas it destabilizes the molten globule state (MG) in the MG-to-D transition. Thus, not only the nature of the protein but also the nature of the structural changes during the transition determines the shape of the P,T-diagram. This rationalizes the apparent discrepancy of our data with those of *Zipp* and *Kauzmann* [17]. These authors observed a N-to-D transition, whereas we observe a N-to-A transition (with A being the aggregate).

What is the origin of the apparent volume increase that causes a conformational transition to be shifted to higher temperatures under pressure? Pressure tends to shift an equilibrium reaction in the direction of the smallest volume [32]. Thus, any reaction accompanied by a volume increase will be opposed by pressure. Cavities arising from imperfect packing of the protein interior and hydration changes are the major factors contributing to ΔV. We put forward the hypothesis that the pressure-induced thermostabilization of myoglobin is due to the positive ΔV associated with the aggregation of myoglobin, *i.e.*, the volume of the aggregate is larger than that of the native state. The aggregation is accompanied by a volume increase because of *i*) the creation of cavities due to the imperfect packing in the interior of the conformationally altered protein molecules; *ii*) the creation of cavities at the intermolecular interfaces of the aggregate, and *iii*) the clustering of hydrophobic side chains in the aggregate, thereby reducing the solvation of these groups and the associated volume decrease. However, pressure-induced thermostabilization is not solely related to protein aggregation, as this effect is also observed under conditions where the conformational changes are reversible [17][40][43]. In those cases, alternative factors are responsible for the positive ΔV. *Hei* and *Clark* [43] suggested that the increased thermal stability of glyceraldehyde-3-phosphate from various thermophiles is correlated to an increased hydrophobicity of the protein. This assumes that the solvation of the hydrophobic groups is accompanied by a volume increase. However, this is still matter of debate, because the organization of water in clathrate-like structures surrounding non-polar groups is expected to result in a volume decrease [45][46]. Nevertheless, hydration can be an important factor, as evidenced from studies on the influence of co-solvents on ΔV [18][47]. *Kunugi* and co-workers [18] were able to show that, for the synthetic homopolymer poly(*N*-ethenyl-2-methylpropanamide), the addition of salts such as sodium sulfate can change the sign of dP/dT at high salt concentrations. This is not necessarily a pure hydration effect, as salts can also induce structural changes and, thus, changes in packing.

More generally, one can state that hydration and cavity properties depend on the type of structural transition occurring due to differences in the solvent-accessible surface area of these states. Thus, the contribution of these variables to ΔV will vary according to the nature of the protein and its transition. Estimates of ΔV on the basis of model systems suggest that ΔV is large and negative. The experimentally observed

small magnitude of ΔV, however, suggests that there is also a positive contribution that, at least in part, compensates for the negative contributions. The origin of this contribution is still the subject of debate [46]. One possible explanation is the existence of the thermal volume, which results from the thermally induced molecular vibrations of both the solute and the solvent molecules, thereby causing an expansion of the solvent volume [48]. At high temperature and moderate pressures, the volume changes due to hydration and the loss of cavities are compensated by the increase in thermal volume, resulting in a less-negative ΔV. This leads to pressure-induced stabilization. Upon further increases in pressure, this is no longer the case, and dP/dT changes sign. In contrast, the changes in thermal volume for proteins such as ribonuclease A cannot counterbalance the hydration and intrinsic volume changes, and ΔV gradually becomes more negative with increasing temperature [49]. Consequently, ribonuclease A is not stabilized against thermal denaturation by pressure.

4. Conclusions. – Thermal scans of myoglobin have been performed at moderate pressures (<100 MPa), and it was observed with IR spectroscopy that pressure stabilizes the protein against aggregation. Subsequent dissociation of the aggregate at higher temperatures enabled the characterization of the heat-denatured state. On the basis of these data, we have proposed an extended state diagram of myoglobin that reflects all possible polypeptide-chain conformations, including the aggregated state. Moreover, in this diagram, the denatured state is no longer considered the same under different *P,T*-conditions. It remains to be seen whether the proposed state diagram is applicable to other proteins.

The results presented in this paper were obtained with the support from the *Research Fund* of the Katholieke Universiteit Leuven, the *Fund for Scientific Research, Flanders* and *COST D30* (WG006-03). *F. M.* is supported by a Marie Curie *Intra-European Fellowship* within the *6th European Community Framework Programme. L. S.* thanks the *Hungarian Fund ETT 545*.

Experimental Part

Sample Preparation. Horse heart myoglobin ($\geq 90\%$ pure) was purchased from *Sigma* (St. Louis, MO, USA) and used without further purification. The protein was dissolved in 10 mM deuterated *Tris*-HCl buffer (pD 7.6) to obtain a concentration of *ca.* 3.5 mM. The protein soln. was stored overnight to ensure sufficient H/D-exchange of all solvent accessible protons.

Temperature Denaturation under Isobaric Conditions. High temperatures were achieved in a *Graseby Specac* (Orpington, UK) variable temp. cell in which the classical temp. cell is replaced with an electrically heated diamond anvil cell (DAC; *Diacell Products*, Leicester, UK). The pressure was increased by means of a membrane that, under pressure from helium gas, pushes the diamond anvils against one another[1]). Barium sulfate was used to monitor the pressure inside the DAC [50]. The temp. increment was 0.5°/min and the cooling rate was 1°/min.

FT-IR. IR Spectra were recorded with a *Bruker IFS-66* FT-IR spectrometer equipped with a liquid-nitrogen-cooled mercury-cadmium-telluride solid-state detector. The sample compartment was continuously purged with dry air; 250 spectra were co-added after registration with a resolution of 2 cm^{-1}.

Resolution enhancement was achieved by *Fourier* self-deconvolution, a mathematical technique of band narrowing, performed with the *Bruker* software. The assumed line shape was Lorentzian. A half bandwidth of 21 cm^{-1} and an enhancement factor of 1.7 were used. The meaning of these parameters has been discussed elsewhere [51].

---

[1]) See http://www.diacellproducts.com/wcm.html.

The secondary structure was determined by fitting the self-deconvoluted amide I band of the spectrum with Gaussian functions. The fitting of component peaks was performed by a program developed in our laboratory based on the *Levenberg – Marquard* algorithm [52].

REFERENCES

[1] R. Ravindra, R. Winter, *ChemPhysChem* **2003**, *4*, 359.
[2] P. W. Bridgman, *J. Chem. Phys.* **1935**, *3*, 597.
[3] G. Tammann, 'Kristallisieren und Schmelzen', Johann Ambrosius Barth, Leipzig, 1903, p. 24.
[4] P. W. Bridgman, *J. Biol. Chem*. **1914**, *19*, 511.
[5] K. Suzuki, *Rev. Phys. Chem. Jpn.* **1960**, *29*, 49.
[6] S. A. Hawley, *Biochemistry* **1971**, *10*, 2436.
[7] J. F. Brandts, in 'Structure and Stability of Biological Macromolecules', Eds. S. N. Timasheff, G. D. Fasman, Marcel Dekker, New York, 1969, Vol. 2, p. 213.
[8] P. Rubens, K. Heremans, *Biopolymers* **2000**, *54*, 524.
[9] C. Hashizume, K. Kimura, R. Hayashi, *Biosci. Biotech. Commun.* **1995**, *59*, 1455.
[10] A. Yayanos, in 'Extremophiles', Eds. K. Horikoshi, W. D. Grant, Wiley-Liss, New York, 1998, p. 47.
[11] S. Kunugi, K. Takano, N. Tanaka, K. Suwa, M. Akasi, *Macromolecules* **1997**, *30*, 4499.
[12] S. Rastogi, G. W. H. Höhne, A. Keller, *Macromolecules* **1999**, *32*, 8897.
[13] B. Wroblowski, J. F. Diaz, K. Heremans, Y. Engelborghs, *Proteins* **1996**, *25*, 446.
[14] G. Hummer, S. Garde, A. E. Garcia, M. E. Paulaitis, L. R. Pratt, *Proc. Natl. Acad. Sci. U.S.A.* **1998**, *95*, 1552.
[15] H. Lesch, H. Stadlbauer, J. Friedrich, J. M. Vanderkooi, *Biophys. J.* **2002**, *82*, 1644.
[16] M. H. Jacob, C. Saudan, G. Holtermann, A. Martin, D. Perl, A. E. Merbach, F. X. Schmid, *J. Mol. Biol.* **2002**, *318*, 837.
[17] A. Zipp, W. Kauzmann, *Biochemistry* **1973**, *12*, 4217.
[18] S. Kunugi, Y. Yamazaki, K. Takano, N. Tanaka, *Langmuir* **1999**, *15*, 4056.
[19] L. Smeller, *Biochim. Biophys. Acta* **2002**, *1595*, 11.
[20] M. Fändrich, C. M. Dobson, *EMBO J.* **2002**, *21*, 5682.
[21] Y. V. Griko, V. P. Kutyshenko, *Biophys. J.* **1994**, *67*, 356.
[22] J. Zhang, X. Peng, A. Jonas, J. Jonas, *Biochemistry* **1995**, *34*, 8631.
[23] J. M. Richardson III, S. D. Lemaire, J.-P. Jacquot, G. I. Makhatadze, *Biochemistry* **2000**, *39*, 11154.
[24] F. Meersman, L. Smeller, K. Heremans, *Biophys. J.* **2002**, *82*, 2635.
[25] D. Eisenberg, W. Kauzmann, 'The Structure and Properties of Water', Oxford University Press, 1969.
[26] A. A. Ismail, H. H. Mantsch, P. T. T. Wong, *Biochim. Biophys. Acta* **1992**, *1121*, 183.
[27] A. Dong, T. W. Randolph, J. F. Carpenter, *J. Biol. Chem*. **2000**, *275*, 27689.
[28] G. Damaschun, H. Damaschun, H. Fabian, K. Gast, R. Krober, M. Wieske, D. Zirwer, *Proteins* **2000**, *39*, 204.
[29] I. E. Holzbaur, A. M. English, A. A. Ismail, *Biochemistry* **1996**, *35*, 5488.
[30] F. Meersman, K. Heremans, *Biochemistry* **2003**, *42*, 14234.
[31] B. M. Gorovits, P. M. Horowitz, *Biochemistry* **1998**, *37*, 6132.
[32] J. L. Silva, D. Foguel, C. A. Royer, *Trends Biochem. Sci.* **2001**, *26*, 612.
[33] D. M. Byler, H. Susi, *Biopolymers* **1986**, *25*, 469.
[34] M. Jackson, H. H. Mantsch, *Crit. Rev. Biochem. Mol. Biol*. **1995**, *30*, 95.
[35] D. Reinstädler, H. Fabian, J. Backmann, D. Naumann, *Biochemistry* **1996**, *35*, 15822.
[36] D. Shortle, *FASEB J.* **1996**, *10*, 27.
[37] K. A. Dill, *Protein Sci*. **1999**, *8*, 1166.
[38] A. Tamura, K. Kimura, K. Akasaka, *Biochemistry* **1991**, *30*, 11313.
[39] A. G. Gittis, W. E. Stites, E. E. Lattman, *J. Mol. Biol.* **1993**, *232*, 718.
[40] D. N. Dubins, R. Filfil, R. B. Macgregor Jr., T. V. Chalikian, *Biochemistry* **2003**, *42*, 8671.
[41] K. A. Dill, D. Stigter, *Adv. Prot. Chem.* **1995**, *46*, 59.
[42] C. Dirix, F. Meersman, C. E. MacPhee, C. M. Dobson, K. Heremans, *J. Mol. Biol.* **2005**, in press.
[43] D. J. Hei, D. S. Clark, *Appl. Environm. Microbiol.* **1994**, *60*, 932.
[44] K. Heremans, *High Pressure Res.* **2004**, *24*, 57.

[45] G. Pappenberger, C. Saudan, M. Becker, A. E. Merbach, T. Kiefhaber, *Proc. Natl. Acad. Sci. U.S.A.* **2000**, *97*, 17.
[46] C. A. Royer, *Biochim. Biophys. Acta* **2002**, *1595*, 201.
[47] H. Herberhold, C. A. Royer, R. Winter, *Biochemistry* **2004**, *43*, 3336.
[48] T. V. Chalikian, K. J. Breslauer, *Biopolymers* **1996**, *39*, 619.
[49] T. Yamaguchi, H. Yamada, K. Akasaka, *J. Mol. Biol*. **1995**, *250*, 689.
[50] P. T. T. Wong, D. J. Moffat, *Appl. Spectrosc*. **1989**, *43*, 1279.
[51] L. Smeller, K. Goossens, K. Heremans, *Appl. Spectrosc*. **1995**, *49*, 1538.
[52] W. H. Press, B. P. Flannery, S. A. Teukolsky, W. T. Vetterling, 'Numerical Recipes: The Art of Scientific Computing', Cambridge University Press, Cambridge, 1986, Chapter 12.6.

Received November 18, 2004